ELECTRONIC SUPPLEMENTARY MATERIAL

ARTICLE TITLE: Deciphering post-caldera volcanism: insight into the Vulcanello (Aeolian Islands, Southern Italy) eruptive activity based on geological and petrological constraints

JOURNAL: Bulletin of Volcanology

AUTHORS: Raffaella Fusillo, Federico Di Traglia, Anna Gioncada, Marco Pistolesi, Paul J. Wallace, Mauro Rosi

CORRESPONDING AUTHOR: Anna Gioncada, Dip. Scienze della Terra, Università di Pisa, Via Santa Maria 53, 56126 Pisa, Italy, gioncada@dst.unipi.it

Methods

Fieldwork and morphological analyses

Field data collection was carried out during different surveys starting from 2008. Forty natural sections were integrated with six machine-excavated and hand-dug pit trenches during the stratigraphic survey of the 1.4 km^2 of Vulcanello peninsula. At each site, a detailed stratigraphic log of the volcanic succession was measured and described. Global positioning system (GPS) coordinates, photos, and field notes were stored in a dedicated geographic information system (GIS) format, on a Digital Terrain Model (DTM, made by Regione Sicilia using LIDAR technique) with 3x3 m pixel resolution.

The volcanic sequence of the basal lava platform and the three 120 m-high volcanic cones were investigated on the basis of morphological features, while the lava and tephra sequences constituting each cone have been further separated based on the presence of erosive unconformities. Eruptive (primary, i.e. all deposits that do not involve temporary erosional reworking of material; Manville et al. 2009) and epiclastic (no deposits directly related to eruptions) units have been

identified on the basis of erosional unconformities, lithological features and geometric organization of the deposits. A comparison between subaerial products and submarine pillow lavas emplaced on the north-eastern sector (2 km offshore of Vulcanello) has also been carried out (see Romagnoli et al. 2013 for sampling details).

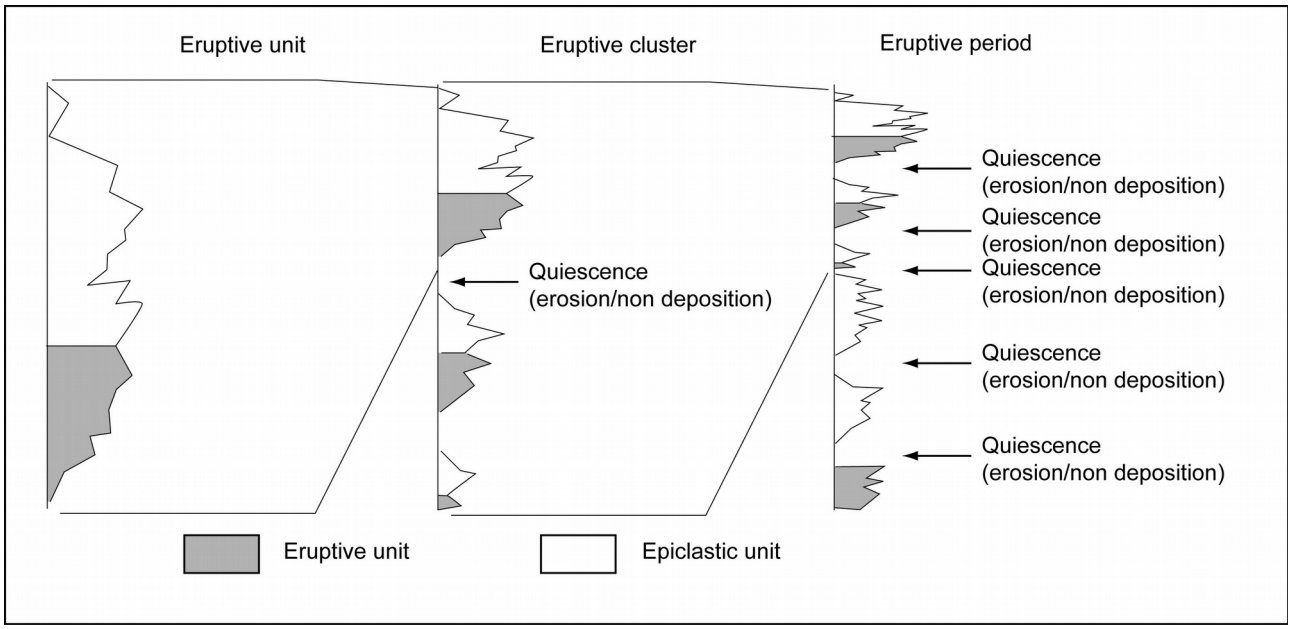

Figure ESM2 - Hierarchization of the stratigraphic units based on the relevance of the unconformities.

Morphological analysis and volume calculations for the Vulcanello peninsula were performed by integrating direct field observations with data from the DTM. The morphological parameters and the boundary between the cones and the surrounding platform were determined using the slope and the profile curvature of the topographic surface, as proposed by Grosse et al. (2009; 2011) and Di Traglia et al. (2013; 2014). As pointed out by Grosse et al. (2012), the profile curvature is the rate of change of slope measured in a vertical plane oriented along the gradient line and thus it directly maps breaks in slope, highlighting both the convexity (positive maxima) and the concavity (negative maxima). The profile curvature and the slope maps were combined in a single data layer (Fig. ESM3) using the following equation (Grosse et al., 2012)

$$Boundary\ delineation\ layer = Profile\ curvature(norm) * f + Slope(norm) * (1 - f) \quad (1)$$

where:

$$Profile\ curvature(norm) = \frac{Profile\ curvature - Profile\ curvature(min)}{Profile\ curvature\ (range)} \quad (2)$$

and:

$$Slope(norm) = \frac{(Slope - Slope(min))^2}{Slope(range)^2} \quad (3)$$

and *f* is a factor ranging from 0 to 1 that weighs each term and depends on the topography of each particular case (Grosse et al., 2012). In this case, a value of 0.5 is considered to better identify the volcanic boundary because this value provides the best view of the cinder cones. The generated layer is used to trace the boundaries by manually searching for the best path along the minimum values of the generated data layer.

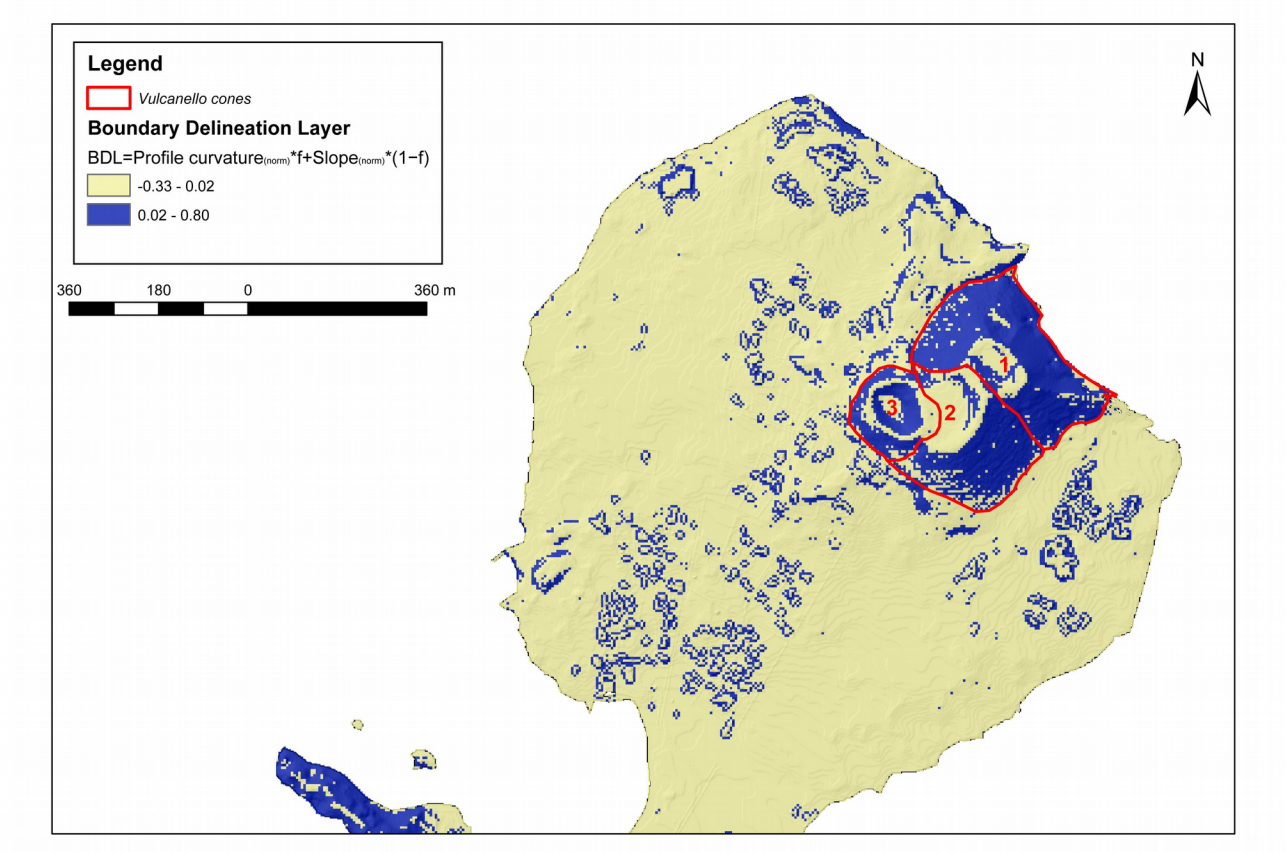

Figure ESM3 - Boundary delineation map obtained from the combination of slope and profile curvature, following Grosse et al. (2009) (see equation in text and figure) that is used to manually trace the Vulcanello cones boundary along the path of minimum values.

Analytical methods

In order to measure the volatile concentrations in olivine-hosted melt inclusions (MI) from rapidly

quenched products of Vulcanello explosive activity, we collected lapilli-sized juvenile clasts from pyroclastic deposits of Vulcanello 1, Vulcanello 2 and Vulcanello 3 lithosomes. We also analysed glass samples from the submarine effusive activity NE of Vulcanello (pillow lava).

Major element compositions of the juvenile clasts were determined by X-ray fluorescence (XRF) spectroscopy at the department of Earth Sciences of the University of Pisa. Infrared spectroscopic analyses of the melt inclusions and glasses were used to measure the dissolved H_2O and CO_2 contents using a ThermoNicolet Nexus 670 spectrometer and Continuum microscope in the Department of Geological Sciences at the University of Oregon. Major elements and F, Cl, and S concentrations were measured in MI, olivine host crystals and pillow lava samples using a Cameca SX-100 electron microprobe in the Lorry I. Lokey Laboratories at University of Oregon.

For each explosive eruptive unit ~300 g of juvenile clasts were crushed using a ceramic mortar for pumices and a jaw crusher for scoriae, and olivine of 0.7 -1.0 mm range size were handpicked. In order to select the crystals with melt inclusions, they were immersed in liquid with refractive index of 1.657. The crystals were then leached in fluoroboric acid (HBF_4) in order to remove the exterior glass and select the samples with the largest and best preserved melt inclusion. Double-polished wafers with both faces intersecting the selected inclusions were prepared.

Infrared spectroscopy analyses were carried out to measure the dissolved H_2O and CO_2 contents of the glasses using a FTIR-Thermo-Nicholet 1000 interfaced with a Spectra-Tech Nic-Planmicroscope in the Department of Geological Sciences at the University of Oregon. A KBr beamsplitter and liquid nitrogen-cooled HgCdTe2 detector were used for all spectra. Total dissolved H_2O (Table 6) was measured from the intensity of the broad, asymmetric peak at 3570 cm^{-1} which corresponds to the fundamental OH^- stretching vibration (Nakamoto 1978; Stolper 1982). The dissolved CO_2 was measured from the intensity of the peak at 1515 e 1430 cm^{-1} corresponding to the antisymmetric stretching of distorted carbonate group (CO_3^{2-}) (Fine and Stolper 1986). Quantitative measurements of dissolved volatile were determined using the Beer's law :

$c = MA/\rho l\epsilon$

where *c* is the concentration by weight of the absorbing species and *M* is its molecular weight (18.02 for total H_2O, molecular H_2O, and OH and 44.00 for CO_3^{2-}). The value of the absorbance, *A,* of the band of interest was calculated from the spectra by the average of three different measurements of the height of the absorption band peak using the OMNIC version 6.0 software. The room density of the glass, ρ, was calculated from major element compositions of analysed MI based on the formulae from R. Lange, as discussed in Luhr (2001) with regard to the value of the partial molar volume for all oxides except TiO_2 e Fe_2O_3. The temperature-dependent partial molar volume for TiO_2 and $Fe_2O_3$are from Lange and Carmichael (1990). The value of the sample thickness, *l,* of each crystal wafer was calculated by the average of three different measurements made by a digital micrometer in three different points before the analysis. The thickness range from a minimum value of 14 microns to a maximum of 269 microns. They were then checked by other three measurements from reflection spectra at each analytical point after the infrared spectroscopy analysis, on the basis of the procedure as reported in Wysoczanski and Tani (2006). The precision of the thickness measurements varies from ± 1 to ± 3 μm. The molar absorption coefficient ϵ, for total dissolved H_2O at the 3570 cm^{-1} band is not strongly dependent on composition (Ihinger et al. 1994), and a value of 63 ±3 l/mol*cm was used (Dobson et al., unpublished data, cited in Dixon et al. 1995). The CO_2 content resulted below the detection limits (~50 ppm) and consequently none molar absorption coefficient was calculated.

EMP analyses of major elements and F, Cl , S concentrations were measured in MI, olivine host crystals and pillow lava samples using a Cameca SX 100 electron microprobe in the Lorry I. Lokey Laboratories at University of Oregon. Olivine host crystals were analyzed using a beam current of 10 nA, electron gun voltage of 15 kV and 10 μm beam diameter, while MI and pillow lava samples were analysed using a beam current of 50 nA, electron gun voltage of 15kV and 10 μm beam diameter. Four to five separates spots were analysed on each MI and pillow lava samples and allowed to verify the homogeneity of the analysed glasses; three separate spots were analysed on each olivine host crystals, close to the MI. The standards included a combination of synthetic

minerals and glass. Sulfur was analysed using a Kα wavelength offset measured on pyrite standard, which corresponds approximately to the $S^{6+}/\Sigma S$ ratio expected for a basaltic glass equilibrated at the FMQ oxygen buffer (Wallace and Carmichael, 1994).

References

Di Traglia F, Morelli S, Casagli N, Garduño Monroy VH (2014) Semi-automatic delimitation of volcanic edifice boundaries: Validation and application to the cinder cones of the Tancitaro–Nueva Italia region (Michoacán–Guanajuato Volcanic Field, Mexico). Geomorphology 219:152-160

Dixon JE, Stolper EM, Holloway JR (1995) An experimental study of water and carbon dioxide solubilities in mid-ocean ridge basaltic liquids. Part I: calibration and solubility models. J Petrol 36:1607–1631

Fine G, Stolper E (1986) Dissolved carbon dioxide in basaltic glasses: concentrations and speciation. Earth Planet Sci Lett 76:263-278

Grosse P, van Wyk de Vries B, Petrinovic IA, Euillades PA, Alvarado G (2009) Morphometry and evolution of arc volcanoes. Geology 37:651–654

Grosse P, van Wyk de Vries B, Euillades PA, Kervyn M, Petrinovic IA (2011) Systematic morphometric characterization of volcanic edifices using digital elevation models. Geomorphology 136:114–131

Ihinger PD, Hervig RL, McMillan PF (1994) Analytical methods for volatiles in glasses. Rev Mineral Geochem 30:67–121

Lange R L, Carmichael I S (1990) Thermodynamic properties of silicate liquids with emphasis on density, thermal expansion and compressibility. Rev Mineral Geochem 24:25-64

Luhr J F (2001) Glass inclusions and melt volatile contents at Paricutin Volcano, Mexico. Contrib Mineral Petrol 142:261-283

Nakamoto K (1978) Infrared and Raman spectra of inorganic and coordination compounds. John Wiley & Sons, Ltd.

Stolper E (1982) The speciation of water in silicate melts. Geochim Cosmochim Acta 46:2609-2620

Wysoczanski RJ, Tani K (2006) Spectroscopic FTIR imaging of water species in silicic volcanic glasses and melt inclusions: an example from the Izu-Bonin arc. J Volcanol Geotherm Res 156:302–314

Wallace P J, Carmichael I S (1994) Petrology of Volcán Tequila, Jalisco, Mexico: disequilibrium phenocryst assemblages and evolution of the subvolcanic magma system. Contrib Mineral Petrol 117: 345-361